scientific reports

OPEN

Peri-coronary adipose tissue attenuation and its association with plaque vulnerability and clinical outcomes in coronary artery disease using combined CCTA and OCT

Caifeng Yang[1,3], Chancui Deng[1,3], Jie Xia[1], Sha Wang[1], Long Zhang[1], Zhijiang Liu[1], Wei Zhang[1], Yi Deng[1], Shiwan Lu[1], Guanxue Xu[2✉] & Bei Shi[1✉]

Vascular inflammation plays a pivotal role in the pathogenesis of atherosclerotic plaques, driving their progression from a stable to an unstable phenotype. Previous research has identified a relationship between peri-coronary adipose tissue (PCAT) attenuation, as assessed by coronary computed tomography angiography (CCTA), and the degree of coronary inflammation, which is associated with an elevated risk of cardiovascular mortality. Nevertheless, the interplay between PCAT attenuation, as determined by CCTA, and plaque characterization via optical coherence tomography (OCT), alongside clinical outcomes, remains inadequately explored. In this study, we retrospectively analyzed data from 111 patients with coronary artery disease who underwent a sequential diagnostic workup comprising CCTA, coronary angiography (CAG), and OCT from January 2022 to May 2023. Patients were stratified into two groups based on a PCAT attenuation threshold of -70.1 Hounsfield units (HU): a high-PCAT attenuation group ($n = 39$) and a low-PCAT attenuation group ($n = 72$). The cohort was further divided into major adverse cardiac event (MACE) and non-MACE groups, depending on whether a MACE occurred during a median follow-up period of 504 days. Compared to the low-PCAT attenuation group, patients in the high-PCAT attenuation group were younger (55.77 ± 9.33 vs. 60.07 ± 9.88; $p < 0.028$) and exhibited a higher incidence of acute coronary syndrome (ACS) (30.8% vs. 13.9%; $p = 0.033$). Additionally, lipid-rich plaques (84.6% vs. 52.8%; $p = 0.001$), macrophages (79.5% vs. 51.4%; $p = 0.004$), thin-cap fibrous atherosclerotic plaques (TCFA) (43.6% vs. 25.0%; $p = 0.044$), and red blood clots (33.3% vs. 15.3%; $p = 0.027$) were more prevalent in the high-attenuation group. Multivariate logistic regression analysis revealed that high PCAT attenuation was an independent predictor of lipid plaques, macrophage presence, and TCFA. During the follow-up period, 22 patients (19.8%) experienced a primary clinical endpoint event. Patients in the MACE group demonstrated higher levels of PCAT attenuation compared to those in the non-MACE group (– 69.67 [– 74.75, – 65.59] HU vs. – 73.67 [– 76.67, – 69.50] HU, $p = 0.037$). Multivariate Cox proportional hazards regression modeling further substantiated that elevated PCAT attenuation was independently associated with an increased risk of MACE. In conclusion, the high-attenuation group exhibited more OCT-detected features indicative of vulnerable plaques and a higher frequency of MACE events relative to the low-attenuation group. These findings suggest a significant association between elevated vascular inflammation, as reflected by PCAT attenuation, vulnerable plaque characteristics identified by OCT, and poorer clinical outcomes.

Keywords Peri-coronary adipose tissue, Optical coherence tomography, Plaque vulnerability, Clinical outcomes

[1]Department of Cardiology, Affiliated Hospital of Zunyi Medical University, Zunyi 563000, China. [2]Department of Cardiology, The Fifth Affiliated Hospital of Zunyi Medical University, Zhuhai, China. [3]Caifeng Yang and Chancui

Deng have contributed equally to this paper and share first authorship. ✉email: xuguanxue2008@163.com; shibei2147@163.com

Vascular inflammation is recognized as one of the key factors in atherosclerotic plaque formation as well as in the progression of coronary heart disease[1]. Recently, a novel non-invasive marker of vascular inflammation has been investigated that detects vascular inflammation by measuring peri-coronary adipose tissue (PCAT) attenuation using coronary computed tomography angiography (CCTA)[2,3]. Previous studies have demonstrated that PCAT attenuation detected by CTAA correlates with coronary artery inflammation, which plays a crucial role in atherosclerotic plaque formation and its progression[2]. Coronary inflammation is captured by mapping the spatial variation of perivascular fat attenuation on CCTA, known as the fat attenuation index (FAI)[4]. FAI captures inflammation-induced variations in perivascular fat attenuation, allowing early detection of coronary inflammation using conventional CCTA, which can reflect the vascular degree of inflammation[5].

Higher lipoprotein(a) levels were associated with increased coronary plaque loading, low-density noncalcified plaques, and increased inflammation in PCAT in a long-term prospective serial CCTA imaging study[6]. Studies have confirmed that the inflammatory response plays a key regulatory role in the development of coronary atherosclerotic plaques. Optical coherence tomography (OCT), with its high-resolution imaging technology, can visually identify the lesion site, allowing detailed assessment of coronary artery lumen size, plaque morphology, degree of stent dilatation, and stent location[7,8]. Notably, there was a significant correlation between the high-risk plaque features detected by CCTA (low-attenuation plaques, punctate calcification) and the vulnerable plaques defined by OCT (thin fibrous cap atheromatous plaques, macrophage infiltration)[9]. This suggests that the intrinsic link between vascular inflammatory status and plaque vulnerability assessed by noninvasive imaging means is of significant clinical value. It was confirmed that elevated PCAT attenuation values calculated based on CCTA were not only significantly associated with increased risk of cardiac death, but also strongly correlated with vulnerable plaque features (thin fibrous cap, macrophage infiltration) detected by OCT[10]. Further analysis showed a significant increase in the incidence of OCT-detected vulnerable plaques in patients in the high PCAT attenuation group compared with the low PCAT attenuation group, suggesting that the vascular inflammatory microenvironment may be involved in cardiovascular events through mechanisms that promote plaque destabilization[11]. By comparing the PCAT values of patients with ruptured plaques to those of patients with plaque erosions, Nakajima[12] found that patients with ruptured plaques had a vascular inflammation levels were significantly higher than those in the plaque erosion group, a finding that is highly consistent with histopathologic evidence and further validates the key role of vascular inflammation in plaque instability. Among patients with suspected coronary artery disease, the PCAT imaging histology model constructed by CCTA can predict whether a MACE event occurs in the future with higher accuracy compared with the FAI model[13]. In the future, a comprehensive model constructed by combining the PCAT imaging model and the FAI model will show more excellent predictive efficacy in identifying the risk of potential MACE events, and is expected to provide a more valuable decision basis for clinical evaluation and intervention.

In summary, existing studies have confirmed the correlation between PCAT attenuation values and the level of vascular inflammation, as well as several studies evaluating the relationship between PCAT and cardiac and vascular-related lesions. However, there is still a lack of systematic research evidence on the relationship between vascular inflammation levels and OCT plaque characteristics and clinical outcomes. Based on the above research background, the present study intends to investigate the association between vascular inflammation levels assessed by PCAT attenuation values based on CCTA and OCT plaque characteristics through a retrospective study design, and to further analyze the predictive efficacy of PCAT attenuation on adverse cardiovascular events in patients with coronary artery disease.

Patients and methods
Patient selection
This study was a retrospective, observational, single-center study. It was not pre-registered on platforms such as ClinicalTrials.gov. This study included 123 patients diagnosed with coronary artery disease at the Department of Cardiovascular Medicine, Zunyi Medical University Hospital. Between January 2022 and May 2023, these patients underwent a series of examinations, including CCTA, coronary angiography (CAG), and OCT. Inclusion Criteria: (1) Diagnosed with acute coronary syndromes (ACS) and stable angina pectoris (SAP). (2) Underwent both CCTA and OCT imaging. (3) Hemodynamically stable at the time of imaging. (4) No contraindications for iodinated contrast or invasive imaging procedures. Exclusion Criteria: (1) History of prior revascularization (percutaneous coronary intervention or coronary artery bypass grafting). (2) Contraindications to iodinated contrast agents. (3) Hemodynamic instability or inability to tolerate imaging procedures. (4) Poor imaging quality or incomplete imaging data. SAP and ACS diagnoses were made following the guidelines set by the American Heart Association/American College of Cardiology[14]. Definitions are provided in **Supplemental Appendix 1**. Among the participants, 3 ST-Elevation Myocardial Infarction (STEMI) patients underwent CCTA an average of 1.6 days before PCI, 9 Non-ST-Elevation Myocardial Infarction (NSTEMI) patients underwent CCTA an average of 36.6 days before PCI, 80 Unstable Angina Pectoris (UAP) patients underwent CCTA an average of 20.9 days before PCI, and 19 SAP patients underwent CCTA an average of 16.1 days before PCI. 111 patients were ultimately enrolled. The PCAT intelligent analysis software (developed by Beijing Shukun Network Technology Co., Ltd., China) was utilized to assess the average attenuation of PCAT in three coronary arteries. Patients were then classified into high and low PCAT attenuation groups based on a threshold of -70.1 HU[5]. The study adhered to the Declaration of Helsinki and was approved by the Ethics Committee of the Affiliated Hospital of Zunyi Medical University. All patients provided written informed consent. Ethics Approval Number: KLLY-2023-142.

CCTA acquisition and PCAT attenuation analysis

CT images were acquired using a Siemens Definition Flash Dual-Source CT (DSCT) machine, adhering to the guidelines set forth by the Society for Cardiovascular Computed Tomography[15]. The area from 1 to 1.5 cm below the tracheal bifurcation to the diaphragmatic surface of the patient's heart was taken as the extent of the scan. Using a German Ulrich high-pressure syringe, 50–65 mL of the contrast agent iohexol was injected intravenously into the patient's median elbow vein at a rate of 4–5 mL/s, followed immediately by 50 ml of saline intravenously at the same rate. To monitor the CT value, a contrast tracer is used at the root level of the aorta using a region of interest (ROI), which is delayed for 7 s and then automatically triggered for scanning once the monitored CT value reaches 100 HU. Cardiac gating technology can be used to automatically set the width of the exposure window according to heart rate, and to set the scanning parameters: scanning layer thickness of 0.75 mm, collimation of 128×0.6 mm, automatic pitch setting (range 0.2 to 0.4), rotation time of 0.28 s, tube voltage of 120 kV, and tube current of 252 to 310 mAs. When the coronary artery reaches the optimal phase for display, i.e., the minimum phase for artefacts, reconstruction of the image begins. All scans were performed in a single breath-hold.

PCAT is defined as the adipose tissue surrounding a coronary artery, extending from the lateral vessel wall over an area equal to the vessel's diameter3[3]. PCAT attenuation represents the average CT attenuation of fat tissue within the defined area, with CT values ranging from – 190 to -30 HU. To assess inflammation levels in the major coronary arteries, the analysis of PCAT around the right coronary artery (RCA) included the segment 10 mm to 50 mm proximal to the vessel, excluding the first 10 mm to avoid partial volume effects and artifacts from intraluminal contrast agents. The left coronary artery system, due to its variable length and potential absence, excluded the left main artery. Measurements were limited to the proximal 40 mm of the left anterior descending (LAD) and left circumflex (LCX) arteries10[16]. Two radiologists with 15 and 20 years of CCTA image interpretation experience selected the clearest imaging sequences of the three major coronary arteries. The CT images of all eligible patients were imported into the intelligent analysis software for the PCAT (Beijing Shukun Network Technology Co., Ltd., China). The software automatically analyzed and calculated the average density of PCAT within the designated regions of interest in the coronary arteries[17]. Representative images of PCAT attenuation are shown in Fig. 1.

OCT analysis

The OCT imaging system employed in this study was the frequency-domain OCT ILUMIEN/ILUMIEN OPTIS (St. Jude Medical, St. Paul, MN, USA). All OCT procedures were conducted by seasoned interventional
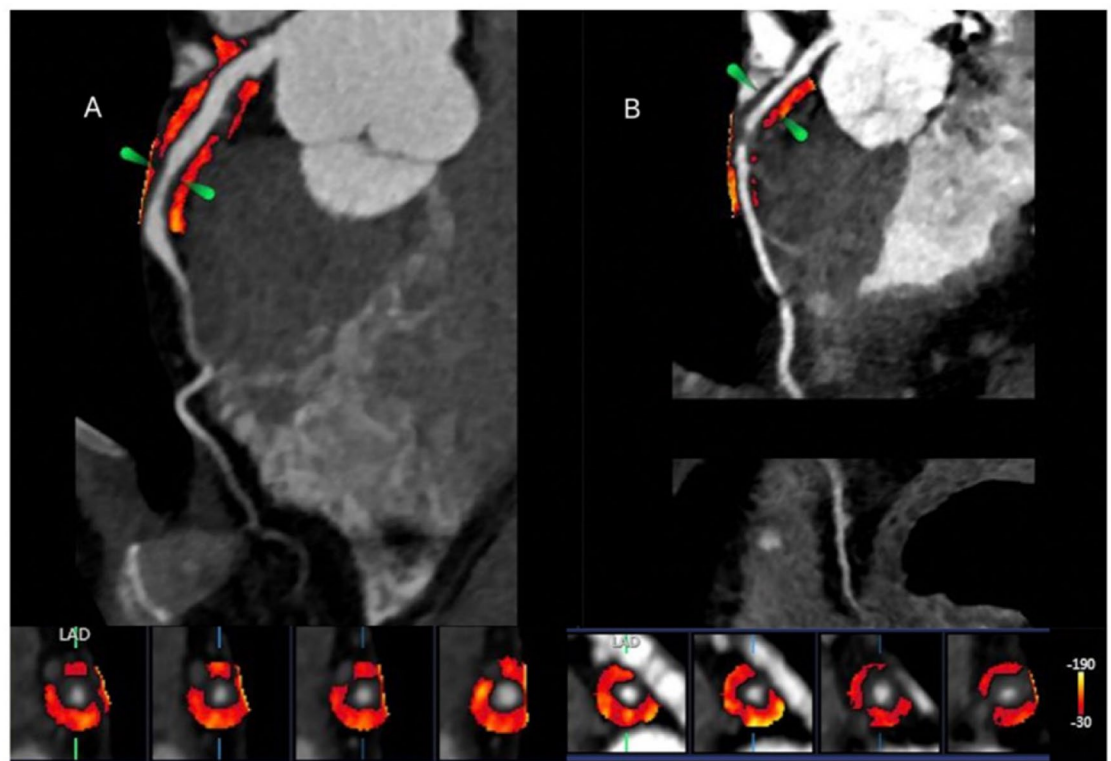

Fig. 1. Two representative images of PCAT attenuation differences between patients with and without MACE measured by CCTA. (**A**) A 57-year-old patient (male) with MACE, the PCAT attenuation was – 70HU. (**B**) A 42-year-old patient (male) without MACE, the PCAT attenuation was – 84HU. CCTA = coronary computed tomography angiography, HU = hounsfield unit, MACE = major adverse cardiovascular event, PCAT = pericoronary adipose tissue.
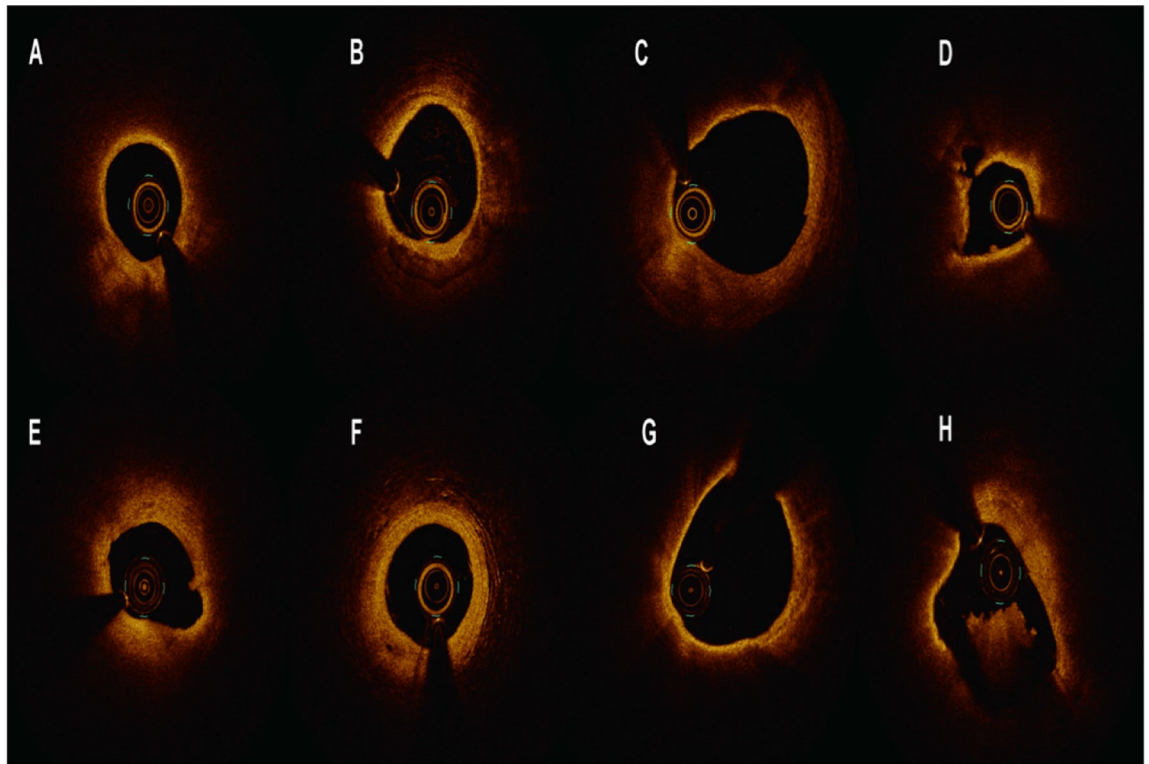
Fig. 2. Representative OCT images are shown in Fig. 2. (**A**) Lipid plaque. (**B**) Calcified plaque. (**C**) TCFA. (**D**) Plaque rupture. (**E**) Plaque erosion. (**F**) NV. (**G**) Macrophages. (**H**) Red thrombus. TCFA = Thin-cap fibrous atherosclerotic, NV = Neovascularization.

cardiologists. A 2.7 F imaging catheter was introduced via a 6–7 F guiding catheter through the radial artery, and the ultrasound catheter was advanced at least 5 mm beyond the target lesion. The automatic pullback speed was set between 10 and 36 mm/s, with a scanning frequency of 100 or 180 frames per second. During the acquisition of OCT images, 3–4 mL/s of contrast agent was injected to clear intravascular blood. All OCT images were stored for offline analysis. Quantitative analysis of the OCT images was performed using Light Lab Imaging Inc. (Westford, MA) software. Prior to analysis, Z-offset calibration was performed, and an OCT cross-sectional image was selected every 1.0 mm (5 frames) of the lesion segment for measurement and analysis. Each selected cross-section was semi-automatically acquired, with all measurement criteria based on the 2012 American College of Cardiology expert consensus on OCT[18]. All OCT images were independently analyzed by two researchers using LightLab OCT software (Light Lab Imaging Inc., Westford, MA, USA), blinded to the angiographic and clinical outcomes. In instances of disagreement between the observers regarding qualitative plaque morphology analysis, a third researcher was consulted to achieve consensus. The diagnostic criteria for OCT plaque (Fig. 2) are provided in **Supplemental Appendix 1.**

Followup and end point
Clinical follow-up data were obtained from hospital visits, outpatient appointments, or phone follow-ups, with a median follow-up period of 504 days. The primary objective of this study was to evaluate major adverse cardiac events (MACE), which included all-cause mortality, recurrent nonfatal myocardial infarction, ischemia-driven revascularization, recurrent angina, and heart failure recurrence post-discharge as a composite endpoint.

Statistical analysis
Statistical analysis was performed using SPSS version 29.0 (IBM SPSS Statistics). The normality of the data was assessed using a one-sample Kolmogorov-Smirnov test. Normally distributed data are expressed as mean ± standard deviation ($\chi \pm s$), with group comparisons conducted using independent sample t-tests. Non-normally distributed data are presented as median [M (Q1, Q3)], with group comparisons performed using the Mann-Whitney U test. Categorical data are presented as percentages, with group comparisons made using the χ^2 test or Fisher's exact test. Univariate and multivariate logistic regression analyses identified independent factors influencing OCT plaque characteristics. Receiver operating characteristic (ROC) analysis classified PCAT attenuation into binary categories, with the optimal threshold determined by the area under the curve (AUC) and the Youden index. Kaplan-Meier survival analysis and Log-rank tests compared survival rates between the high and low attenuation groups. Univariate and multivariate Cox proportional hazards regression analyses evaluated factors influencing MACE. Predictors with a univariate p-value < 0.10 were included in multivariate logistic and Cox regression models. Collinearity diagnostics assessed the collinearity between variables in

multivariate models. Collinearity was considered absent if the variance inflation factor (VIF) was less than 10, and highly correlated variables were excluded from multivariate regression analysis. The kappa coefficient assessed the intra-group and inter-group consistency of qualitative OCT data. Statistical significance was defined as a two-tailed p-value < 0.05.

Results

Baseline patient characteristics

Flowchart showing the study design Fig. 3. Baseline characteristics (Table 1). This study included 111 patients with coronary artery disease, with a mean age of 58.56 ± 9.87 years, 78 patients (70.3%) were male. Among the cohort, 61 patients (55.0%) had hypertension, 27 patients (24.3%) had diabetes, and 63 patients (56.8%) were current smokers. Younger patients were more prevalent in the high attenuation group. A total of 22 patients (19.8%) were admitted with acute ACS, while 89 patients (80.2%) were admitted with SAP. The high attenuation group had a greater proportion of ACS patients, whereas the low attenuation group had a higher proportion of SAP patients. A comparison of PCAT attenuation levels between ACS and SAP patients (**Supplementary Figure S1**) demonstrated that ACS patients had significantly higher PCAT attenuation, achieving statistical significance. While patients in the high attenuation group exhibited numerically lower ejection fractions (61.00 [57.25–62.00] vs. 60.00 [56.00–62.00]; $p = 0.225$) and higher CRP levels (20.01 [2.57–69.61] vs. 14.19 [0.99–69.61]; $p = 0.270$), these differences were not statistically significant.

OCT findings

An analysis of PCAT attenuation was conducted using both quantitative and qualitative OCT data (Table 2), comparing the plaque characteristics between the high and low PCAT attenuation groups. In quantitative analysis, the high PCAT attenuation group exhibited significantly smaller minimum lumen area (MLA) (1.42 [0.89-2.00] vs. 1.89 [1.32–2.67]; $p = 0.011$) and minimum lumen diameter (MLD) (1.33 [1.06–1.55] vs. 1.52 [1.28–1.82]; $p = 0.002$) compared to the low PCAT attenuation group. Additionally, the high PCAT attenuation group showed a higher percentage of minimum lumen diameter stenosis (58.90 [54.80–65.30] vs. 54.55 [47.48–60.13]; $p = 0.003$) and minimum lumen area stenosis (83.40 [78.84–88.50] vs. 78.85 [71.83–84.88]; $p = 0.001$), as well as thinner fibrous cap thickness (FCT) (60.00 [50.00–70.00] vs. 90.00 [60.00-137.50]; $p = 0.000$).In qualitative analysis, the high PCAT attenuation group demonstrated a significantly higher prevalence of lipid-rich plaques [33 (84.6%) vs. 38 (52.8%); $p = 0.001$], macrophage infiltration [31 (79.5%) vs. 37 (51.4%); $p = 0.004$], red thrombi [13 (33.3%) vs. 11 (15.3%); $p = 0.027$], and TCFA [17 (43.6%) vs. 18 (25.0%); $p = 0.044$] compared to the low PCAT attenuation group (**Supplementary Figure S2**). Furthermore, a detailed assessment of PCAT
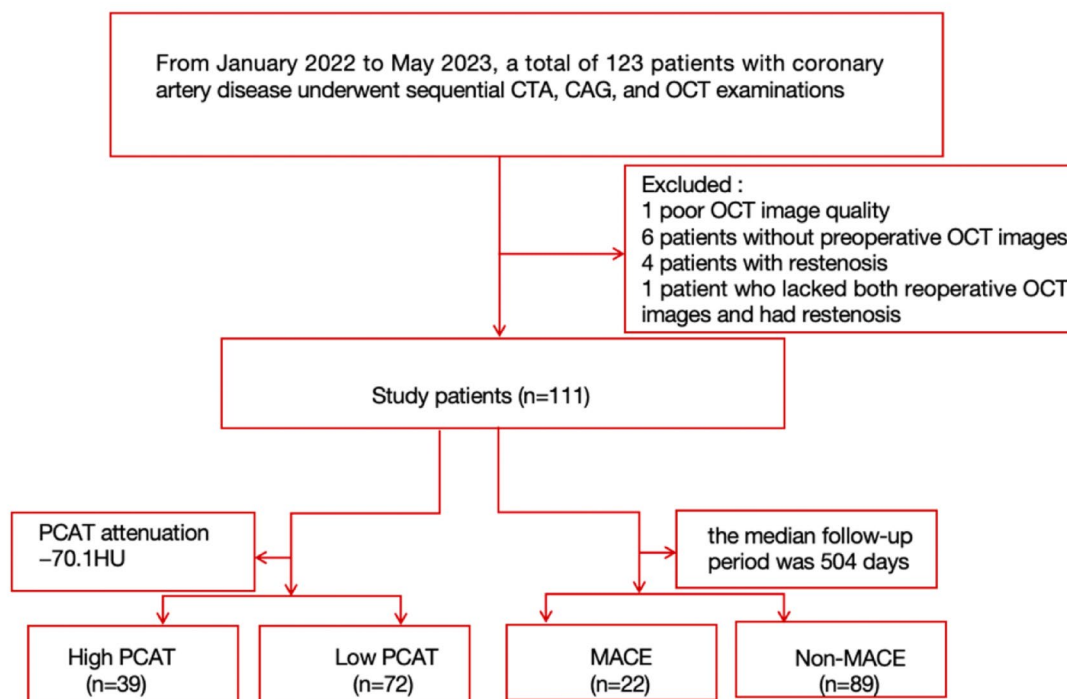

Fig. 3. Flowchart showing the study design. CAG = Coronary Arteriography, CCTA = coronary computed tomography angiography, MACE = major adverse cardiac events, OCT = Optical coherence tomography, PCAT = peri-coronary adipose tissue.

	Overall (*n* = 111)	High PCAT attenuation group	Low PCAT attenuation group	*p*-value
General information				
Age, year	58.56 ± 9.87	55.77 ± 9.33	60.07 ± 9.88	0.028
Male, n (%)	78 (70.3)	29 (74.4)	49 (68.1)	0.488
Current smoker, n (%)	63 (56.8)	25 (64.1)	38 (52.8)	0.250
Hypertension, n (%)	61 (55.0)	24 (61.5)	37 (51.4)	0.305
Diabetes mellitus, n (%)	27 (24.3)	10 (25.6)	17 (23.6)	0.812
LVEF, %	60 (57–62)	60.00 (56.00–62.00)	61.00 (57.25-62.00)	0.225
Creatinine, μmol/L	76 (66–85)	76.00 (79.00–86.00)	74.00 (62.50-83.75)	0.202
eGFR, mL/min/1.73 m^2	92.41 (75.24–107)	88.64 (72.84-107.66)	92.94 (75.69-106.52)	0.539
TG, mmol/L	1.80 (1.29–3.25)	1.94 (1.40–3.67)	1.79 (1.23–2.86)	0.367
TC, mmol/L	5.01 (4.20–5.71)	5.18 (4.22–5.97)	4.92 (4.18–5.67)	0.201
HDL-C, mmol/L	1.19 ± 0.25	1.17 ± 0.23	1.20 ± 0.26	0.470
LDL-C, mmol/L	3.02 (2.38–3.5)	3.04 (2.49–3.56)	2.99 (2.24–3.40)	0.406
WBC (×10^9/L)	6.38 (5.73–7.91)	6.41 (5.37–8.20)	6.37 (5.38–7.78)	0.643
CRP (mg/L)	20.01 (1.26–69.61)	20.01 (2.57–69.61)	14.19 (0.99–69.61)	0.270
Neu (×10^9/L)	4.00 (3.35–5.13)	4.04 (3.35–5.32)	3.80 (3.35–4.89)	0.505
Lym (×10^9/L)	1.68 (1.29–2.08)	1.65 (1.29–2.13)	1.68 (1.26–2.06)	0.998
NT-pro BNP, pg/mL	72.00 (30.00-214.00)	66.00 (27.00-383.00)	77.00 (33.00-213.75)	0.767
Clinical presentation				
SAP, n (%)	89 (80.2)	27 (69.2)	62 (86.1)	0.033
ACS, n (%)	22 (19.8)	12 (30.8)	10 (13.9)	
Medication				
Aspirin, n (%)	73 (65.8)	27 (69.2)	46 (63.9)	0.571
Statin, n (%)	111 (100)	39 (100)	39 (100)	
ACEI/ARB, n (%)	65 (58.6)	23 (59.0)	42 (58.3)	0.948
β-blocker, n (%)	100 (90.1)	35 (89.7)	65 (90.3)	1.000
Antiplatelet, n (%)	107 (96.4)	38 (97.4)	69 (95.8)	1.000

Table 1. Baseline characteristics. ACS = acute coronary syndrome, ACEI = angiotensin-converting enzyme inhibitor, ARB = angiotensin II receptor blocker, CRP = high-sensitivity C-reactive protein, eGFR = estimated glomerular filtration rate, HDL-C = high-density lipoprotein cholesterol, LVEF = left ventricular ejection fraction, Lym = lymphocyte, LDL-C = low-density lipoprotein cholesterol, NT-proBNP = N-terminal pro-brain natriuretic peptide, Neu = neutrophils, SAP = stable angina pectoris, TG = Triglyceride, TC = total cholesterol; Values are mean ± SD, n (%), or median (25th–75th percentile), WBC = white blood cell.

attenuation based on different OCT plaque characteristics (Fig. 4) consistently revealed that the presence of TCFA, lipid plaques, and macrophages was associated with significantly higher coronary PCAT attenuation, all achieving statistical significance. No statistically significant difference in red thrombus incidence was observed between the two groups, although a higher incidence was noted in the high PCAT attenuation group.

Univariate and multivariate logistic analysis of OCT plaque characteristics

Univariate and multivariate logistic regression analyses were conducted to compare the effects of various factors on OCT plaque characteristics, focusing on three aspects: lipid plaques, macrophages, and TCFA. First, univariate and multivariate logistic regression analyses were conducted on lipid plaques in all study participants (**Supplementary Table S1**). The univariate analysis revealed that higher PCAT attenuation (OR: 4.92; 95% CI [1.84, 13.18], *p* = 0.002) was associated with an increased incidence of lipid plaques. Including univariate predictors with a p-value < 0.10 in the multivariate logistic regression analysis further showed that higher PCAT attenuation (OR: 4.40; 95% CI [1.77, 10.93], *p* = 0.001), Hypertension (OR: 3.07; 95% CI [1.21, 7.79], *p* = 0.018) and LDL-C (OR: 2.07; 95% CI [1.12, 3.81], *p* = 0.020) were significantly correlated with the presence of lipid plaques. Additionally, univariate and multivariate logistic regression analyses were performed on the macrophage population in each patient (**Supplementary Table S2**). The univariate analysis showed that higher PCAT attenuation (OR: 3.67; 95% CI [1.48, 9.05], *p* = 0.005) was independently associated with the presence of macrophages. Further multivariate logistic regression analysis confirmed that higher PCAT attenuation remained significantly correlated with the presence of macrophages (OR: 3.31; 95% CI [1.28, 8.55], *p* = 0.014). Finally, univariate and multivariate logistic regression analyses were performed to assess the occurrence of TCFA in all patients (**Supplementary Table S3**). The univariate analysis revealed that higher PCAT attenuation(OR: 5.14; 95% CI [2.27, 11.67], *p* = 0.000), TC (OR: 1.59; 95% CI [1.10, 2.30], *p* = 0.013), AS%MLD (OR: 1.05; 95% CI [1.01, 1.09], *p* = 0.044),and LDL-C (OR: 1.77; 95% CI [1.06, 2.97], *p* = 0.030) were associated with a higher occurrence of TCFA. The multivariate Cox regression analysis identified high PCAT attenuation (OR: 4.22;

	Overall (*n* = 111)	High PCAT attenuation	Low PCAT attenuation	*p*-value
Quantitative analysis				
MLA, mm^2	1.74 (1.12–2.51)	1.42 (0.89-2.00)	1.89 (1.32–2.67)	0.011
MLD, mm	1.45 (1.18–1.75)	1.33 (1.06–1.55)	1.52 (1.28–1.82)	0.002
AS % (MLD site)	57 (49.45–62.85)	58.90 (54.80–65.30)	54.55 (47.48–60.13)	0.003
AS % (MLA site)	81.2 (73.9-86.25)	83.40 (78.84–88.50)	78.85 (71.83–84.88)	0.001
Thinnest FCT, mm	70 (60–120)	60.00 (50.00–70.00)	90.00 (60.00-137.50)	0.000
Max lipid arc, °	230 (180–300)	230.00 (180.00-300.00)	222.55 (172.50–300.00)	0.425
Lipid length, mm	9.1 (6.65–11.65)	10.20 (6.90–13.30)	9.10 (6.45–11.35)	0.141
Qualitative analysis				
Macrophages, n (%)	68 (61.3)	31 (79.5)	37 (51.4)	0.004
Microvessels, n (%)	66 (59.5)	26 (66.7)	40 (55.6)	0.255
TCFA, n (%)	35 (31.5)	17 (43.6)	18 (25.0)	0.044
Lipid plaques, n (%)	71 (64.0)	33 (84.6)	38 (52.8)	0.001
Calcification, n (%)	38 (34.2)	12 (30.8)	26 (36.1)	0.571
Red thrombus, n (%)	24 (21.6)	13 (33.3)	11 (15.3)	0.027
White thrombus, n (%)	21 (18.9)	9 (23.1)	12 (16.7)	0.410
Plaque Rupture, n (%)	23 (20.7)	11 (28.2)	12 (16.7)	0.152
Plaque Erosion, n (%)	46 (41.4)	18 (46.2)	28 (38.9)	0.458

Table 2. Optical coherence tomography characteristics. FCT = fibrous cap thickness, MLD = Minimum lumen diameter, MLA = Minimum lumen area, OCT = optical coherence tomography, PCAT = peri-coronary adipose tissue, TCFA = thin-cap fibroatheroma, Values are mean ± SD, n (%), or median (25th–75th percentile).
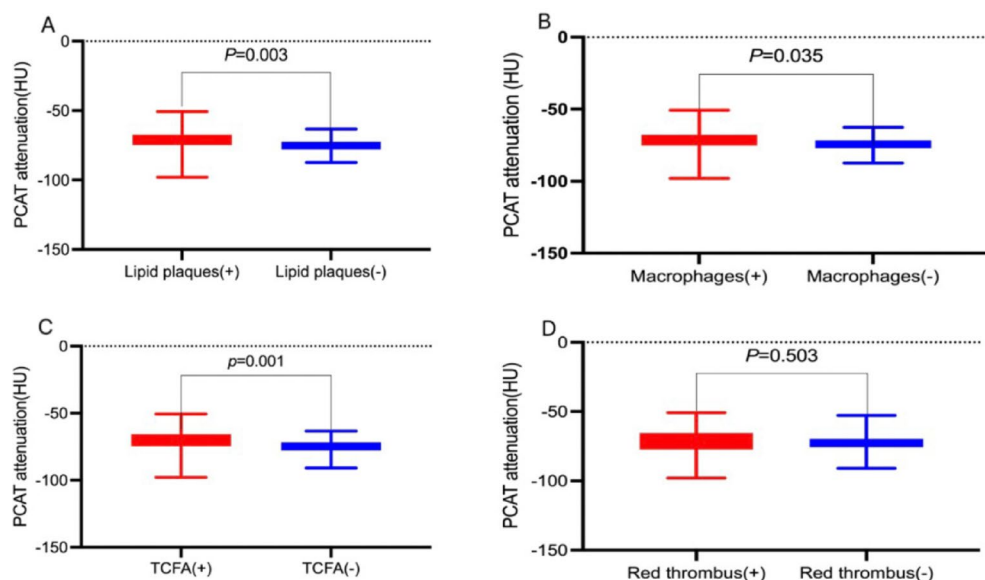

Fig. 4. Differences on PCAT attenuation between optical coherence tomography plaque. (**A**). PCAT attenuation was significantly higher in patients with lipid plaque (+) than in those with lipid plaque (-). (**B**). PCAT attenuation was significantly higher in patients with Macrophages (+) than in those with Macrophages (-). (**C**). PCAT attenuation was significantly higher in patients with TCFA (+) than in those with TCFA (-). (**D**). PCAT attenuation showed no statistically significant difference between the two groups regarding red thrombus; however, there was an observable trend towards an increase in the incidence of red thrombus in the high attenuation group. Student's t-test was applied to obtain P values. PCAT = peri-coronary adipose tissue, TCFA = thin-cap fibroatheroma.
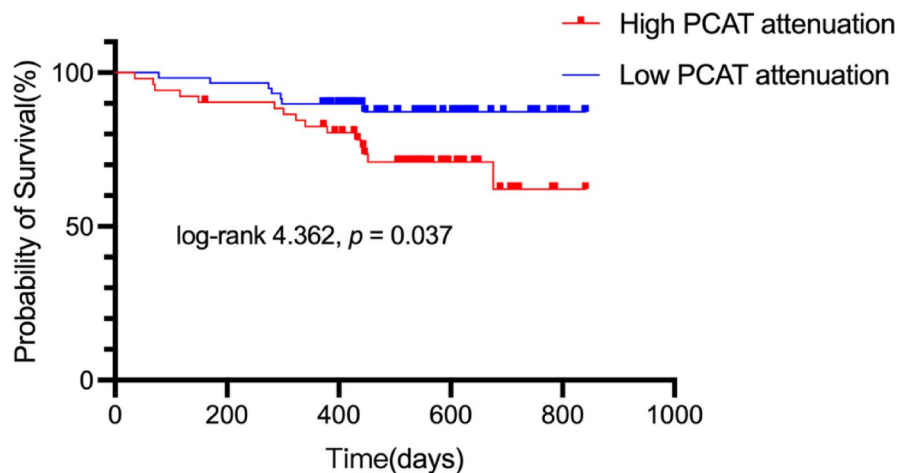
Fig. 5. Kaplan-Meier curves for the primary outcome of major adverse cardiovascular events.

95% CI [1.68, 10.57], $p = 0.002$) and hypertension (OR: 3.05; 95% CI [1.20, 7.74], $p = 0.019$) as significant factors associated with TCFA incidence.

Clinical outcome

In this study, the median follow-up period was 504 days, during which 22 patients (19.82%) experienced MACE. These included 7 cases of heart failure recurrence, 12 cases of recurrent UAP, 2 cases of NSTEMI, and 1 case of non-cardiac death. Patients were categorized into two groups based on the occurrence of MACE during the follow-up period: those who experienced MACE and those who did not. The clinical baseline characteristics of both groups are presented in **Supplementary Table S4**, with relevant definitions and diagnostic criteria available in **Supplemental Appendix 1**. The Kaplan-Meier curve for the primary endpoint is presented in Fig. 5. In the high PCAT attenuation group, the primary endpoint occurred in 12 patients (30.8%), whereas in the low PCAT attenuation group, 10 patients (13.9%) reached the primary endpoint (**Supplementary Table S5**). Comparison of MACE incidence between the two groups revealed a higher event probability in the high PCAT attenuation group. Analysis of the differences in PCAT attenuation between the MACE and non-MACE groups (**Supplementary Figure S3**) showed that PCAT attenuation was significantly higher in the MACE group. Additionally, heart failure was significantly more prevalent in the high PCAT attenuation group than in the low PCAT attenuation group. The ROC curve indicated that the cutoff value for PCAT attenuation in predicting MACE was − 72.84 HU (**Supplementary Figure S4**).

Predictors of the incidence of MACE

In this study, univariate and multivariate Cox proportional hazards regression analyses were conducted to assess the occurrence of MACE in the study population (**Supplementary Table S6**). The univariate analysis revealed that increased PCAT attenuation (HR: 2.46; 95% CI [1.06, 5.70], $p = 0.036$), severe stenosis (HR: 6.93; 95% CI [2.12, 22.57], $p = 0.004$), and WBC (HR, 1.13; 95% CI [1.03, 1.24]; $p = 0.008$) were associated with the occurrence of MACE. After including univariate predictors with p-values < 0.10 in the multivariate logistic regression model, the results indicated that high PCAT attenuation (HR, 2.41; 95% CI [1.02, 5.69]; $p = 0.045$), WBC (HR, 1.12; 95% CI [1.02, 1.23]; $p = 0.018$) and severe luminal stenosis (HR, 6.67; 95% CI [2.23, 19.99]; $p = 0.000$) were risk factors for MACE.

Reproducibility of qualitative OCT analysis

The kappa coefficients for inter-observer and intra-observer consistency in the qualitative OCT analysis for lipid plaques, macrophages, and TCFA were 0.922/0.940, 0.848/0.885, and 0.814/0.835, respectively.

Discussion

This study presents several key findings: (1) Compared to the low attenuation group, the high attenuation group had a higher prevalence of lipid plaques, macrophages, and TCFA; (2) After adjusting for coronary plaque factors, high PCAT attenuation remained a significant determinant of lipid plaques, macrophages, and TCFA; (3) The incidence of MACE was significantly higher in the high attenuation group, potentially reflecting a worse prognosis for patients with coronary artery disease. Even after controlling for factors affecting MACE, high PCAT attenuation was still an independent predictor of MACE. These results suggest that high PCAT attenuation is linked to plaque vulnerability and significantly impacts the clinical outcomes of coronary artery disease patients, highlighting its critical role in the pathogenesis and progression of the disease.

Vascular inflammation plays a pivotal role in both the formation of atherosclerotic plaques and the destabilization of existing plaques. Initially, immune cells activate inflammatory cells such as macrophages, mast cells, and neutrophils. These inflammatory mediators trigger the production of reactive oxygen species, leading to the oxidation of low-density lipoprotein (LDL). Macrophages engulf oxidized LDL, transforming into

foam cells and initiating plaque formation. Consequently, immune and inflammatory cells are predominant in the early stages of atherosclerosis, with their inflammatory factors promoting plaque progression[19]. Research indicates that elevated levels of plasma inflammatory biomarkers, such as interleukin-6 (IL-6), are associated with cardiovascular events, and that implementing anti-inflammatory strategies can reduce the occurrence of adverse cardiovascular events[20]. Key pro-inflammatory factors released by inflammatory cells include tumor necrosis factor-α (TNF-α), IL-6, and interferon-γ (IFN-γ), which induce vasoconstriction, stimulate the migration and proliferation of smooth muscle cells, and promote oxidative stress[21]. Under the stimulation of these inflammatory mediators, the proliferation and differentiation of preadipocytes in PCAT are inhibited, resulting in the formation of low-lipid, high-water adipocytes. This unique alteration can be visualized on CCTA as spatial changes in coronary artery fat attenuation[9,21]. PCAT attenuation is depicted in red regions (Fig. 1), thereby allowing the assessment of vascular inflammation through PCAT attenuation[22].

Recent studies have demonstrated that high PCAT attenuation is linked to vulnerable plaques identified via OCT[11], high-risk plaques observed on CCTA[10], the progression of non-culprit lesion plaques[23], and elevated cardiac mortality[5]. Our analysis examined the relationship between PCAT attenuation and OCT plaque characteristics, finding a higher prevalence of lipid plaques, macrophages, and TCFA in the high PCAT attenuation group. After adjusting for relevant factors, high PCAT attenuation remained a significant predictor of lipid plaques, macrophages, and TCFA. This correlation suggests that high PCAT attenuation is linked to traditional plaque characteristics, including TCFA, lipid plaques, and macrophages, and may serve as a novel marker for identifying high-risk plaques. These results suggest that higher PCAT attenuation is associated with poorer clinical outcomes, which may reflect its role in the pathogenesis and progression of coronary artery disease. No significant correlation was found between red thrombus and PCAT attenuation, nor was a significant impact of OCT plaque characteristics on clinical outcomes observed. This may be attributed to the limited sample size and the single-center study design. To validate these findings, future research should include larger, prospective, multicenter studies, as well as further investigations to determine whether higher PCAT attenuation is associated with plaque instability.

Recent studies have shown that high PCAT attenuation, assessed by CCTA prior to PCI, is significantly correlated with a reduced coronary flow reserve 1 month post-PCI[24]. This finding suggests that PCAT attenuation could help identify high-risk coronary artery disease (CAD) patients at greater risk of future cardiac events[25]. In this study, the incidence of MACE was significantly higher in the high attenuation group. Multivariate Cox regression analysis revealed that PCAT attenuation (HR, 2.41; 95% CI [1.02, 5.69]; $p = 0.045$) influenced the occurrence of MACE. Severe stenosis and WBC were also identified as a contributing factor. Therefore, future studies should combine these factors to predict adverse cardiovascular events in CAD patients. Studies suggest that PCAT accumulation may lead to microvascular obstruction, influencing the prognosis of heart failure patients[26]. Indeed, most events in our study were heart failure-related, supporting the idea that high PCAT attenuation causes microcirculatory disturbances and indicates increased inflammation and fibrosis in PCAT, potentially leading to cardiovascular diseases like heart failure. Although no statistically significant differences were observed, trends toward lower ejection fractions in the high attenuation group suggest that further investigation with a larger sample size may be warranted to explore the potential clinical implications of these findings.

In his study[27], Makoto Araki showed that ACS patients had significantly higher PCAT attenuation in culprit plaques and vessels than those with SAP. This suggests that vascular inflammation plays a key role in the onset of ACS. Other studies also show higher inflammation levels in culprit lesions[28]. Our study supports these findings, with the high attenuation group having more ACS patients, and the low attenuation group having more SAP patients. Moreover, ACS patients exhibited higher PCAT attenuation than SAP patients, emphasizing the role of vascular inflammation in ACS progression. Early anti-inflammatory therapy could help reduce the adverse cardiovascular events linked to elevated PCAT attenuation in CAD patients. Subsequent research should further examine the use of statins or anti-inflammatory treatments and their association with lower PCAT attenuation[29]. High-dose statin therapy has been shown to significantly reduce CAD risk[29]. Blood sugar control may be linked to coronary artery inflammation, as assessed by PCAT attenuation[30]. A recent study found that diabetic patients had significantly higher PCAT attenuation in the right coronary artery (RCA) than non-diabetic patients, regardless of plaque vulnerability or stenosis severity[31]. Li, Y., and colleagues examined the relationship between FAI and Semaglutide treatment in type 2 diabetes patients, multivariate regression analysis revealed a negative correlation between Semaglutide treatment and coronary artery inflammation[32]. In patients with higher lesion-specific PCAT attenuation, intensified anti-inflammatory therapy could reduce MACE incidence[33]. Thus, in the future, PCAT attenuation may serve as a new marker for cardiovascular event risk. Accurate assessment of coronary artery inflammation can assist in developing anti-inflammatory treatment plans and enable risk stratification for CAD patients. Early intervention may help reduce adverse cardiovascular events, improving patient prognosis.

Limitations

First, the study was conducted at a single facility with a small sample size, necessitating further confirmation through larger, multicenter studies. Second, the analysis focused on coronary artery disease patients who underwent both CCTA and CAG. Patients without significant blockages on CCTA may have been excluded from invasive procedures, potentially introducing selection bias. Third, although we observed recurrent heart failure events as part of MACE, the retrospective nature of this study did not allow for a detailed breakdown into ischemic/nonischemic etiologies or HFrEF/HFpEF categories, given that some patients were unable to return to the hospital for follow-up for a variety of reasons and the lack of systematic echocardiographic follow-up data in this group of cases. Future prospective studies should incorporate a standardized classification framework for

heart failure to improve clinical translation. Finally, this study did not examine the association between PCAT attenuation and NSTEMI, STEMI, and MACE events, which could be further refined in future studies.

Conclusions

This study shows that increased vascular inflammation is linked to plaque vulnerability observed on OCT and the overall prognosis of patients with coronary artery disease. Timely and effective anti-inflammatory treatment may improve clinical outcomes in these patients.

Data availability

The datasets used and/or analyzed during this study can be obtained from the corresponding authors upon reasonable request.

References

1. Ross, R. Atherosclerosis–an inflammatory disease. *N Engl. J. Med.* **340**, 115–126. https://doi.org/10.1056/nejm199901143400207 (1999).
2. Antonopoulos, A. S. et al. Detecting human coronary inflammation by imaging perivascular fat. *Sci. Transl Med.* **9** https://doi.org/10.1126/scitranslmed.aal2658 (2017).
3. Antoniades, C., Antonopoulos, A. S. & Deanfield, J. Imaging residual inflammatory cardiovascular risk. *Eur. Heart J.* **41**, 748–758. https://doi.org/10.1093/eurheartj/ehz474 (2020).
4. Dweck, M. R., Fayad, Z. A. & Imaging Perivascular fat - an unheralded informant of coronary inflammation. *Nat. Rev. Cardiol.* **14**, 573–574. https://doi.org/10.1038/nrcardio.2017.127 (2017).
5. Oikonomou, E. K. et al. Non-invasive detection of coronary inflammation using computed tomography and prediction of residual cardiovascular risk (the CRISP CT study): a post-hoc analysis of prospective outcome data. *Lancet* **392**, 929–939. https://doi.org/10.1016/s0140-6736(18)31114-0 (2018).
6. Nurmohamed, N. S. et al. Lipoprotein(a) and Long-Term plaque progression, Low-Density plaque, and pericoronary inflammation. *JAMA Cardiol.* **9**, 826–834. https://doi.org/10.1001/jamacardio.2024.1874 (2024).
7. Araki, M. et al. Optical coherence tomography in coronary atherosclerosis assessment and intervention. *Nat. Rev. Cardiol.* **19**, 684–703. https://doi.org/10.1038/s41569-022-00687-9 (2022).
8. Räber, L. et al. Clinical use of intracoronary imaging. Part 1: guidance and optimization of coronary interventions. An expert consensus document of the European Association of Percutaneous Cardiovascular Interventions. *EuroIntervention* 14, 656–677 (2018). https://doi.org/10.4244/eijy18m06_01
9. Kinoshita, D. et al. High-Risk plaques on coronary computed tomography angiography: correlation with optical coherence tomography. *JACC Cardiovasc. Imaging.* **17**, 382–391. https://doi.org/10.1016/j.jcmg.2023.08.005 (2024).
10. Goeller, M. et al. Pericoronary adipose tissue computed tomography Attenuation and High-Risk plaque characteristics in acute coronary syndrome compared with stable coronary artery disease. *JAMA Cardiol.* **3**, 858–863. https://doi.org/10.1001/jamacardio.2018.1997 (2018).
11. Yuki, H. et al. Coronary inflammation and plaque vulnerability: A coronary computed tomography and optical coherence tomography study. *Circ. Cardiovasc. Imaging.* **16**, e014959. https://doi.org/10.1161/circimaging.122.014959 (2023).
12. Nakajima, A. et al. Plaque rupture, compared with plaque erosion, is associated with a higher level of Pancoronary inflammation. *JACC Cardiovasc. Imaging.* **15**, 828–839. https://doi.org/10.1016/j.jcmg.2021.10.014 (2022).
13. 吴月, 张新伟 & 邢艳 基于CCTA的冠状动脉周围脂肪组织影像组学对不良心血管事件的预测价值. 临床放射学杂志 43, 941–946 (2024). https://doi.org/10.13437/j.cnki.jcr.2024.06.023
14. Kolh, P. et al. 2014 ESC/EACTS guidelines on myocardial revascularization: the task force on myocardial revascularization of the European society of cardiology (ESC) and the European association for Cardio-Thoracic surgery (EACTS). Developed with the special contribution of the European association of percutaneous cardiovascular interventions (EAPCI). *Eur. J. Cardiothorac. Surg.* **46**, 517–592. https://doi.org/10.1093/ejcts/ezu366 (2014).
15. Abbara, S. et al. SCCT guidelines for the performance and acquisition of coronary computed tomographic angiography: A report of the society of cardiovascular computed tomography guidelines committee: endorsed by the North American society for cardiovascular imaging (NASCI). *J. Cardiovasc. Comput. Tomogr.* **10**, 435–449. https://doi.org/10.1016/j.jcct.2016.10.002 (2016).
16. van Diemen, P. A. et al. Prognostic value of RCA pericoronary adipose tissue CT-Attenuation beyond High-Risk plaques, plaque volume, and ischemia. *JACC Cardiovasc. Imaging.* **14**, 1598–1610. https://doi.org/10.1016/j.jcmg.2021.02.026 (2021).
17. Lin, A. et al. Pericoronary adipose tissue computed tomography Attenuation distinguishes different stages of coronary artery disease: a cross-sectional study. *Eur. Heart J. Cardiovasc. Imaging.* **22**, 298–306. https://doi.org/10.1093/ehjci/jeaa224 (2021).
18. Tearney, G. J. et al. Consensus standards for acquisition, measurement, and reporting of intravascular optical coherence tomography studies: a report from the international working group for intravascular optical coherence tomography standardization and validation. *J. Am. Coll. Cardiol.* **59**, 1058–1072. https://doi.org/10.1016/j.jacc.2011.09.079 (2012).
19. Hansson, G. K. Inflammation, atherosclerosis, and coronary artery disease. *N. Engl. J. Med.* **352**, 1685–1695. https://doi.org/10.1056/NEJMra043430 (2005).
20. Broch, K. et al. Randomized trial of Interleukin-6 receptor Inhibition in patients with acute ST-Segment elevation myocardial infarction. *J. Am. Coll. Cardiol.* **77**, 1845–1855. https://doi.org/10.1016/j.jacc.2021.02.049 (2021).
21. Antoniades, C. & Shirodaria, C. Detecting coronary inflammation with perivascular fat Attenuation imaging: making sense from perivascular Attenuation maps. *JACC Cardiovasc. Imaging.* **12**, 2011–2014. https://doi.org/10.1016/j.jcmg.2018.12.024 (2019).
22. Antoniades, C., Kotanidis, C. P. & Berman, D. S. State-of-the-art review Article. Atherosclerosis affecting fat: what can we learn by imaging perivascular adipose tissue? *J. Cardiovasc. Comput. Tomogr.* **13**, 288–296. https://doi.org/10.1016/j.jcct.2019.03.006 (2019).
23. Goeller, M. et al. Relationship between changes in pericoronary adipose tissue Attenuation and coronary plaque burden quantified from coronary computed tomography angiography. *Eur. Heart J. Cardiovasc. Imaging.* **20**, 636–643. https://doi.org/10.1093/ehjci/jez013 (2019).
24. Kanaji, Y. et al. Pre-percutaneous coronary intervention pericoronary adipose tissue Attenuation evaluated by computed tomography predicts global coronary flow reserve after urgent revascularization in patients with Non-ST-Segment-Elevation acute coronary syndrome. *J. Am. Heart Assoc.* **9**, e016504. https://doi.org/10.1161/jaha.120.016504 (2020).
25. Wen, D. et al. Lack of incremental prognostic value of pericoronary adipose tissue computed tomography Attenuation beyond coronary artery disease reporting and data system for major adverse cardiovascular events in patients with acute chest pain. *Circ. Cardiovasc. Imaging.* **16**, 536–544. https://doi.org/10.1161/circimaging.122.015120 (2023).

26. Liu, C. et al. The role of CCTA-derived cardiac structure and function analysis in the prediction of readmission in nonischemic heart failure. *J. Cardiovasc. Transl Res.* **17**, 216–226. https://doi.org/10.1007/s12265-023-10467-6 (2024).
27. Araki, M. et al. Level of vascular inflammation is higher in acute coronary syndromes compared with chronic coronary disease. *Circ. Cardiovasc. Imaging.* **15**, e014191. https://doi.org/10.1161/circimaging.122.014191 (2022).
28. Kuneman, J. H. et al. Pericoronary adipose tissue Attenuation in patients with acute coronary syndrome versus stable coronary artery disease. *Circ. Cardiovasc. Imaging.* **16**, e014672. https://doi.org/10.1161/circimaging.122.014672 (2023).
29. Mátyás, B. B. et al. Assessing the impact of Long-Term High-Dose Statin treatment on pericoronary inflammation and plaque Distribution-A comprehensive coronary CTA Follow-Up study. *Int. J. Mol. Sci.* **25** https://doi.org/10.3390/ijms25031700 (2024).
30. Liu, Y. et al. Coronary inflammation based on pericoronary adipose tissue Attenuation in type 2 diabetic mellitus: effect of diabetes management. *Cardiovasc. Diabetol.* **23**, 108. https://doi.org/10.1186/s12933-024-02199-x (2024).
31. Yu, Y. et al. Increased coronary pericoronary adipose tissue Attenuation in diabetic patients compared to non-diabetic controls: A propensity score matching analysis. *J. Cardiovasc. Comput. Tomogr.* **16**, 327–335. https://doi.org/10.1016/j.jcct.2022.01.002 (2022).
32. Li, Y. et al. Association of semaglutide treatment with coronary artery inflammation in type 2 diabetes mellitus patients: a retrospective study based on pericoronary adipose tissue Attenuation. *Cardiovasc. Diabetol.* **23**, 348. https://doi.org/10.1186/s12933-024-02445-2 (2024).
33. Elnabawi, Y. A. et al. Association of biologic therapy with coronary inflammation in patients with psoriasis as assessed by perivascular fat Attenuation index. *JAMA Cardiol.* **4**, 885–891. https://doi.org/10.1001/jamacardio.2019.2589 (2019).

Acknowledgements

Author contributions

Caifeng Yang and Chancui Deng were responsible for the study design and manuscript writing. Bei Shi, Guanxue Xu, revised the manuscript. Jie Xia, Sha Wang, Long Zhang, Zhijiang Liu, Wei Zhang, Yi Deng, Shiwan Lu were responsible for data acquisition. All authors have read and approved the final manuscript.

Funding

Declarations

Competing interests

The authors declare that they have no known competing financial interests or personal relationships that could have appeared to influence the work reported in this paper.

Ethical approval

The protocol was approved by the Ethics Committee of the Affiliated Hospital of Zunyi Medical University.

Consent to participate

Informed consent was obtained from all individual participants included in the study.

Additional information

Supplementary Information The online version contains supplementary material available at https://doi.org/10.1038/s41598-025-00023-4.

Correspondence and requests for materials should be addressed to G.X. or B.S.

Reprints and permissions information is available at www.nature.com/reprints.

Publisher's note Springer Nature remains neutral with regard to jurisdictional claims in published maps and institutional affiliations.